Available online at www.sciencedirect.com
ScienceDirect
Ceramics International 37 (2011) 3329–3334
CERAMICS INTERNATIONAL
www.elsevier.com/locate/ceramint

# Calcination and associated structural modifications in boehmite and their influence on high temperature densification of alumina

Padmaja Parameswaran Nampi *, Swapankumar Ghosh, Krishna Gopakumar Warrier

*Materials and Minerals Division, National Institute for Interdisciplinary Science & Technology (NIIST), CSIR, Trivandrum 695019, Kerala, India*

Received 29 November 2010; received in revised form 8 March 2011; accepted 7 April 2011
Available online 1 June 2011

**Abstract**

A systematic study is reported on the calcination of boehmite and its associated structural changes, and their effect on densification features. Boehmite precursor gels have been calcined in the temperature range 250–1200 °C. The associated structural changes are identified by FTIR and XRD. The specific surface area measurements indicated a relatively high value of 169 $m^2$/g for boehmite calcined at 400 °C; this value reduced to 4 $m^2$/g on calcination at 1200 °C. In the temperature range 400–1000 °C, the coordination of aluminium changes from a quasioctahedral to a tetrahedral nature, which reverts to octahedral at 1200 °C. The precursor containing γ-alumina gives a 92.1% theoretical density, on sintering at 1500 °C due to the highly unstable quasioctahedral coordination. Boehmite precursors calcined at 400 °C and 1000 °C produced a density of 88.2% and 96.9%, respectively, in the sintered compact at 1500 °C. Boehmite calcined to α-alumina (1200 °C) possesses an octahedral structure having a density of 97.6% at 1500 °C.


*Keywords:* Sol–gel process; A. Calcination; B. Porosity; D. $Al_2O_3$; Densification

## 1. Introduction

The sol–gel technique for the preparation of ceramic precursors offers a variety of advantages over conventional ceramic processing in terms of lower processing and sintering temperatures, as well as fine-grained microstructures [1]. Sol–gel boehmite is a common precursor for the preparation of alumina-based ceramics, composites and catalysts [2–4]. The structure of boehmite, as well as its variation with respect to various synthesis procedures, has been investigated using solid state NMR spectroscopy [5–7]. When heated, boehmite gel undergoes changes such as dehydration, dehydroxylation and the formation of a number of transitional alumina phases leading finally to stable α-alumina phase [8–15]. The transformation of boehmite to γ-alumina at around 500 °C is not accompanied by shrinkage in volume and, therefore, results in a relatively porous structure possessing high specific surface area [16]. The whole process of dehydroxylation of boehmite is associated with a total volume reduction of about 35% and this results in constrained densification when a boehmite–alumina mixture is used for the fabrication of porous alumina ceramics [17]. The different phases of alumina formed during calcination of boehmite are used in various applications. While γ-alumina is used as solid acid catalysts, α-alumina is the preferred phase in high-temperature structural applications. X-ray diffraction (XRD) technique along with FTIR, neutron scattering and NMR has been employed to identify and characterize these phases [18–22]. The dehydroxylation of boehmite gel and formation of different transitional alumina phases are widely reported [19]. In addition, sintering and densification of boehmite precursor gels have been investigated [23,24]. Addition of nucleating seeds is one of the ways of obtaining low temperature α-alumina phase from boehmite [25]. A report by Bahlawane and Watanabe indicated the possibility of obtaining the α-alumina phase directly from boehmite at 950 °C, when starting from a non-aqueous precursor [26]. It is reasonably well understood that densification steps of alumina are correlated with the loss of hydroxyl groups [27]. Therefore calcination and dehydroxylation conditions have a definite

* Corresponding author. Present address: Bioceramics Laboratory, Biomedical Technology Wing, Sree Chitra Tirunal Institute for Medical Sciences and Technology, Trivandrum, Kerala, India. Tel.: +91 471 2520240; fax: +91 471 2341814.
*E-mail addresses:* padmavasudev@gmail.com, padmaja@sctimst.ac.in (P.P. Nampi).

0272-8842/$36.00 
doi:10.1016/j.ceramint.2011.04.129

influence on the sintering behavior of the resultant aluminium oxide [24,28]. Calcination of boehmite precursor involves structural transformation among the various metastable transitional alumina phases, which should have a bearing on the densification of alumina. However, detailed information on the effect of calcination temperature on the structural changes in boehmite, surface area properties and densification behavior of alumina thus obtained, is not reported. In the present paper, boehmite precursor synthesised by an aqueous sol–gel route is calcined at different temperatures and the effect of associated structural changes in high temperature densification is reported.

## 2. Experimental

Boehmite sol was prepared by dispersing 20 g boehmite powder (Condea Chemie, GmbH, Germany) in 1.2 l distilled water and peptizing it with 10% $HNO_3$ to a stable sol at pH 3 followed by ageing at 30 °C for 24 h. The sol was concentrated on a water bath to a viscous state and dried under controlled conditions of 72% relative humidity (RH) at 45 °C. The translucent flat gel pieces obtained on drying were calcined at 250 °C for 5 h to remove gel water. These calcined pieces were powdered and about 1 g dry calcined powder each were calcined at 400, 600, 800, 1000, 1050, 1100 and 1200 °C at a heating rate of 5 °C/min in a programmable furnace (Nabertherm, Germany) with a soaking for 3 h at the peak temperatures. Circular pellets were made from the calcined boehmite by applying a uniaxial pressure of 150 MPa and are denoted as $P_{400}$, $P_{600}$, $P_{800}$, $P_{1000}$, $P_{1050}$, $P_{1100}$ and $P_{1200}$. All the pellets were sintered at 1400 and 1500 °C over a soaking period of 3 h. The densities of the pellets were determined by Archimedes' method. The X-ray diffraction patterns of all the calcined samples were recorded using a Philips PW1710 diffractometer with Cu Kα radiation and Ni filter. The crystallite sizes ($D_{XRD}$) of crystalline phases of boehmite were calculated from the X-ray line broadening by applying full-width-half-maximum ($\beta$) of highest intensity peak to the Scherrer formula [29] given in Eq. (1).

$$D_{XRD} = \frac{0.9\lambda}{\beta \cos\theta} \quad (1)$$

where λ is the wavelength of incident X-ray, and $\theta$ the diffraction angle for the (4 0 0) plane for γ-$Al_2O_3$, (4 0 0) for δ-$Al_2O_3$ and (1 1 3) in the case of α-$Al_2O_3$. Thermal decomposition behavior of boehmite gel was monitored by DTA (Shimadzu 50H, Japan) at a heating rate of 10 °C/min. The FTIR spectra of the boehmite and calcined boehmite samples as KBr pellets were taken in Nicolet Magna-560 Infrared Spectrometer in the wavenumber range 400–4000 $cm^{-1}$. The BET surface area of boehmite and calcined boehmite samples were measured using a Gemini Surface Area Analyser (Model-2360, Micromeritics, USA) by the nitrogen adsorption method after degassing them at 200 °C for 5 h under flowing nitrogen. The scanning electron micrographs (SEM) of a few selected fractured samples were taken by a JEOL JSM 5600LV Scanning Electron Microscope.

## 3. Results and discussion

The differential thermal analysis pattern of the boehmite precursor gel is presented in Fig. 1. The DTA indicates an endotherm at ~440 °C due to the formation of γ-$Al_2O_3$ [30]. The final conversion to crystalline α-$Al_2O_3$ at about 1130 °C is indicated by a small broad exothermic peak. The phase formation and the structural aspects in the calcined powders were monitored by X-ray diffraction and infrared spectroscopy. The X-ray diffraction patterns of dried gel, gel calcined at 400, 900, 1000 and 1200 °C are given in Fig. 2. The boehmite gel dried at 72% RH and 45 °C, gave a characteristic pattern of moderate crystalline boehmite phase (Fig. 2a). The 400 °C calcined sample produced a mixed boehmite and γ-$Al_2O_3$ phase giving a comparatively less crystalline pattern (Fig. 2b). Calcination at 900 °C (Fig. 2c) produced a mainly amorphous sample, but with the presence of a poorly crystalline component of the δ-$Al_2O_3$. At 1000 °C, the δ-$Al_2O_3$ phase becomes sharper with the onset of a θ-$Al_2O_3$ transformation (Fig. 2d). At 1200 °C, highly crystalline α-$Al_2O_3$ phase is observed (Fig. 2e). Calculation from Scherrer equation shows γ-alumina has crystallite size of 7 ± 2 nm. The crystallite size of δ-alumina was 15 ± 2.5 nm, while the α-alumina had a crystallite size of 33 ± 0.5 nm (Fig. 3).

The thermal transformation sequence for boehmite [26] as evident from XRD patterns and as reported earlier is given in Fig. 4.

The variation in specific surface area and pore volume of boehmite calcined at different temperatures is given in Fig. 5. The specific surface area of the dried gel was 139 $m^2/g$ which increased to 173 and 169 $m^2/g$ on calcination at 250 and 400 °C, respectively. On calcination at 250 °C, removal of unbound water and some structural hydroxyl groups results in high surface area, but the value is rather low when compared to the same reported by Lu et al., where a surface area value of 460 $m^2/g$ at 80 °C has been observed [31]. Boehmite contains adsorbed water on the grains and interlayer water in the crystal

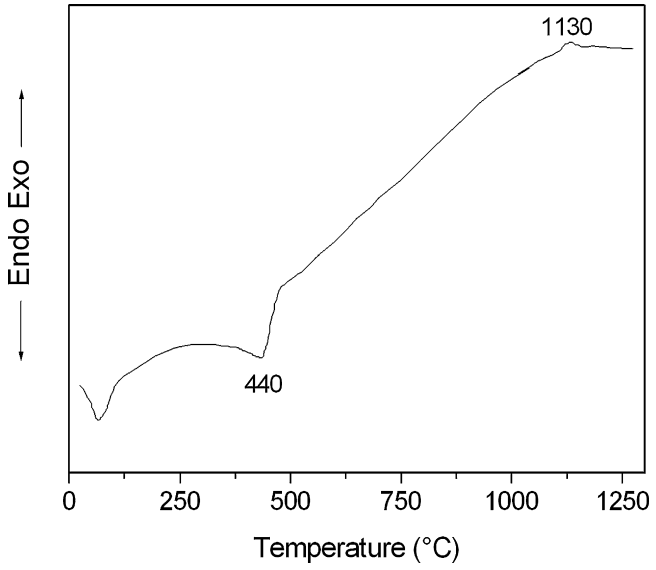


Fig. 1. DTA pattern of boehmite gel.

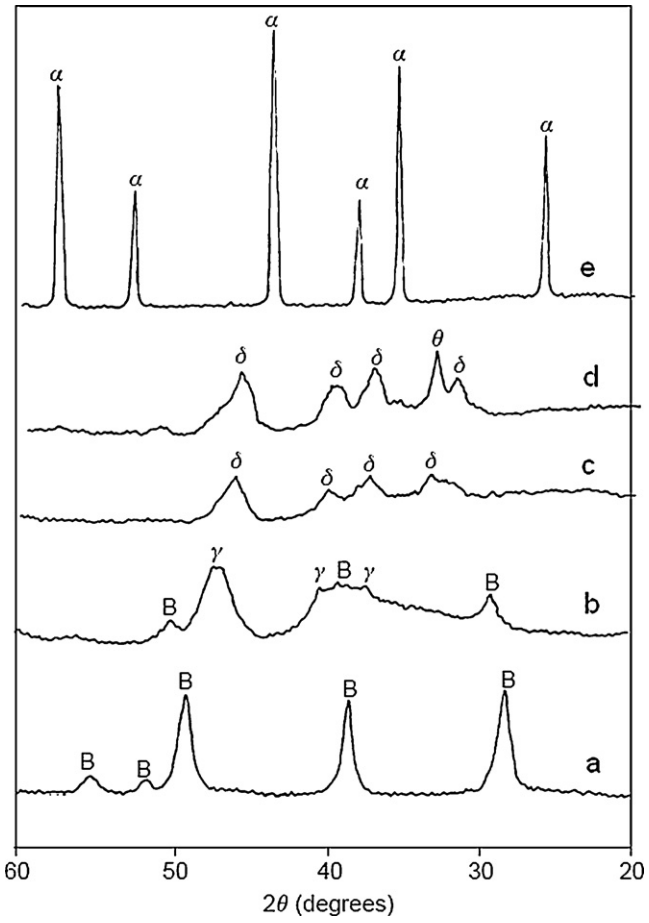


Fig. 2. X-ray diffraction patterns of gel (a) as dried, and gel calcined at (b) 400 °C; (c) 900 °C; (d) 1000 °C; and (e) 1200 °C.

structure. Furthermore, two types of hydroxyl group were also reported in the crystal structure of boehmite and transitional aluminas, one of which dehydrates during the conversion of boehmite into γ-$Al_2O_3$ at around 500 °C, another remains in γ-

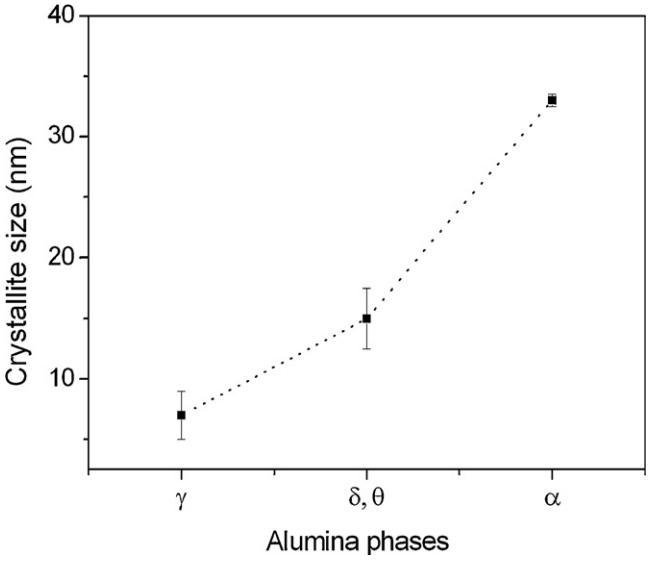


Fig. 3. Crystallite sizes of various alumina phases (γ) γ-$Al_2O_3$; (δ) δ-$Al_2O_3$; (θ) θ-$Al_2O_3$; and (α) α-$Al_2O_3$ using Scherrer equation.

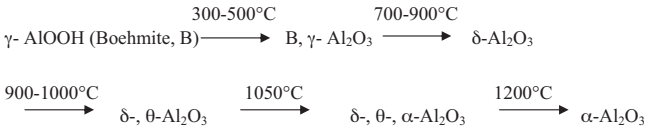


Fig. 4. Thermal transformation sequences for boehmite.

$Al_2O_3$, being gradually lost on further heating [31]. At 400 °C, the hydrogen bonds in the gel disintegrate and minute crystallites of γ-$Al_2O_3$ start forming, thereby causing less reduction in specific surface area. On further increasing the calcination temperature from 400 °C to 600 °C, the nucleation and growth process of γ-$Al_2O_3$ continues and the precursor becomes rich in γ-$Al_2O_3$. The specific surface area of calcined gel is not changed appreciably until the temperature 400 °C is reached. The slight reduction of BET surface area at 400 °C is due to initiation of grain growth with associated reduction in surface energy. In the temperature range 400–1000 °C pore coalescence caused by the collapse of porous structure results in the progressive reduction in specific surface area, as well as pore volume, leading to particle coarsening [28]. The transitional alumina phases, such as δ-, θ-$Al_2O_3$ start forming at around 900 °C. At 1050 °C, α-$Al_2O_3$ phase formation is initiated and at 1200 °C, the transformation is complete resulting in grain coarsening with a subsequent reduction in specific surface area.

FTIR spectra of boehmite samples calcined at 250, 400, 900, 1000 and 1200 °C are given in Fig. 6. The FTIR studies indicate that the gel has only octahedral coordination [19]. The $\nu$-$AlO_6$ and $\nu$-$AlO_4$ peaks, reported in the region 500–750 $cm^{-1}$ and 750–850 $cm^{-1}$, respectively, [19] are observed in the spectra (Fig. 6) with small shifts. The absorption band due to the Al–O–H bending mode is observed at ~1138 $cm^{-1}$ in $P_{400}$ though it is expected in the 900–1100 $cm^{-1}$ range. The stretching modes at 3097 and 3292 $cm^{-1}$ (not shown here) are due to $\nu_s$(Al)OH and $\nu_{as}$(Al)OH stretching vibrations. The shifting of Al–O–H bond stretching frequencies towards lower frequency and bending modes towards higher frequency from the reported values suggested that the boehmite gel is highly hydrogen bonded

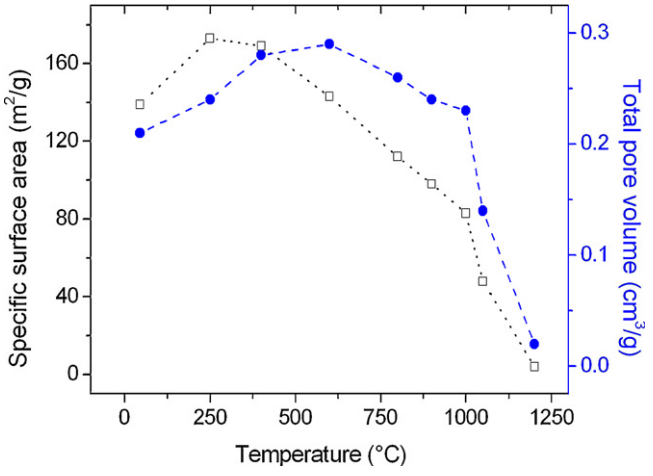


Fig. 5. Variation in specific surface area (empty squares) and pore volume (filled circles) of boehmite as a function of temperature of calcination.

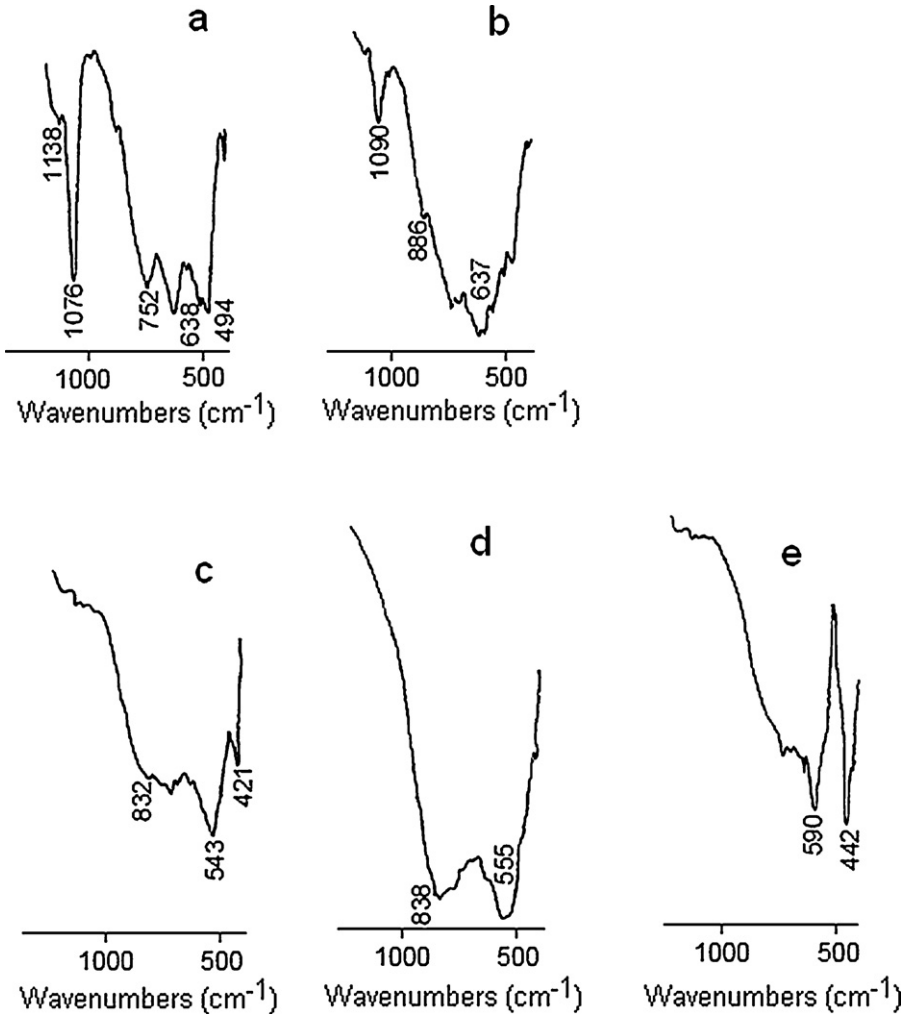


Fig. 6. FTIR spectra of boehmite gel calcined at temperatures (a) 250 °C; (b) 400 °C; (c) 900 °C; (d) 1000 °C; and (e) 1200 °C.

[19]. At 400 °C, the $Al^{3+}$ cation exists in tetrahedral and quasioctahedral coordination in γ-$Al_2O_3$ [16]. In the temperature range 700–1000 °C, aluminium exists in tetrahedral and octahedral/quasioctahedral coordination in δ-$Al_2O_3$ and θ-$Al_2O_3$ [16]. Quasioctahedral represents a coordination state in which the Al is on the way to octahedral through tetrahedral and tetragonal distortion stages. In the powder calcined at higher temperatures (above 900 °C), the relative intensity of absorption at ~830 $cm^{-1}$ due to ν-$AlO_4$ decreases, indicating that aluminium moves towards octahedral coordination. Sharpening of the absorption peaks (Fig. 6) at higher temperatures as a result of the increased structural ordering is evident in the transitional alumina transformation sequence [32]. At 1200 °C, the $AlO_6$ stretching and bending modes get sharper and split into two peaks at 590 and 442 $cm^{-1}$ indicating the formation of a corundum phase (α-$Al_2O_3$).

Densities of samples $P_{400}$, $P_{600}$, $P_{800}$, $P_{1000}$, $P_{1050}$, $P_{1100}$ and $P_{1200}$, sintered at 1400 °C and 1500 °C, are presented in Fig. 7. There is a constant improvement in density on sintering as the calcination temperature of the boehmite precursor is increased

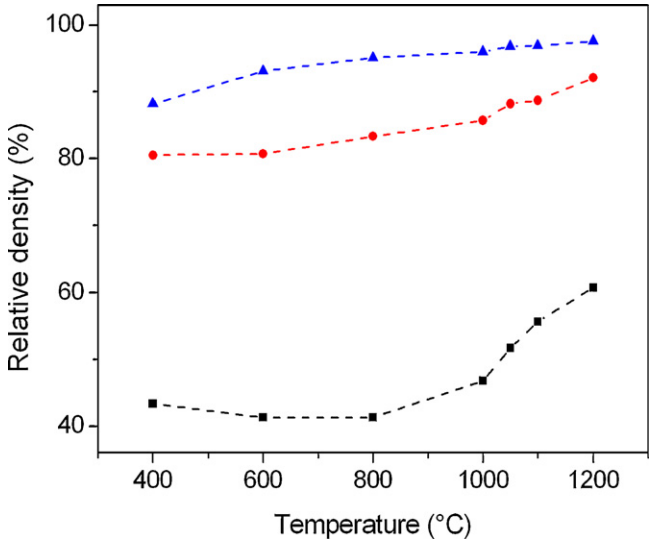


Fig. 7. Variation of % theoretical density of as compacted cylindrical samples (squares), sintered at 1400 °C (circles) and 1500 °C (triangles) as a function of calcination temperatures.

from 400 to 1200 °C at both the sintering temperatures. Sample $P_{400}$ gives a density of 80.5% on sintering at 1400 °C. The density gradually increases to 92.1% when the calcination temperature is 1200 °C ($P_{1200}$) under identical conditions. The density of $P_{1200}$ increases to 97.6% as the sintering temperature is further increased to 1500 °C. Calcination of boehmite gel above 250 °C destroys only the boehmite surface hydroxyls leaving the structural oxygen layers unaffected. At 400 °C, the gel is partially dehydroxylated [19]. As dehydroxylation proceeds, more and more surfaces are produced with highly unstable cationic species and at 600 °C, almost all the OH species escape resulting in the complete formation of γ-$Al_2O_3$ [16]. There is a marked improvement in density from 88.2% to 93.1% on sintering $P_{400}$ and $P_{600}$ at 1500 °C. The presence of γ-$Al_2O_3$ helps the sintering process of alumina by providing additional nucleation sites [33]. Highly unstable cations in γ- and δ-$Al_2O_3$ have high mobility and they contribute to aluminium cation diffusion sintering [16]. The unit cell of γ-$Al_2O_3$ is considered to be made up of skeletal oxygen layers which remain intact after the OH layers of the boehmite precursor are broken down. This leaves a cell with initially empty inter-skeletal layer regions. Short range ordering occurs within the unit cell whereby cations migrate into site positions within the inter-skeletal layers. The atoms within these regions will be rather disordered initially but increasingly become ordered as the structure evolves with higher temperature treatment. More atoms migrate into the inter-skeletal layers as the structure evolves, with the proportion of octahedrally and tetrahedrally coordinated aluminium remaining constant. It is this migration of ions which help in the process of sintering. A new transitional phase, γ′-$Al_2O_3$, has been identified by Paglia et al. [12] which may be considered as a series of transition states within the γ- to θ-$Al_2O_3$ transformation. The cation ordering is more obvious in this structure of γ′-$Al_2O_3$ (with fewer site positions being occupied with increasing calcination temperature) [31]. It is reported that the increase in tetragonal distortion of γ′-$Al_2O_3$ coincided with the migration of vacancies to octahedral positions [12]. The tetragonal distortions in γ- and δ-$Al_2O_3$ coincide with the vacancy ordering on tetrahedral and octahedral sites, respectively, and the change in the tetragonal distortion relates to the cation migration between the sites. The cations in the octahedral sites are considerably disordered, which is a consequence of the rapid change in the structure of γ′-$Al_2O_3$ with increasing temperature of treatment [12]. These disordered cation migrations enhance diffusion sintering. On further increase of calcination temperature, the density of the sintered product (at 1500 °C) is improved only marginally. However, above 1050 °C, transitional alumina transforms into α-$Al_2O_3$ where all the aluminium cations are octahedrally coordinated in three dimensions into compact particles; hence, there is sintering to dense (97.6% theoretical density) product by volume diffusion. It is seen that boehmite as well as α-$Al_2O_3$ has $Al^{3+}$ in octahedral coordination, but exists in different crystal structures [19]. Samples containing a boehmite phase have lower density compared to one containing α-$Al_2O_3$. This is due to hydroxyl ions which form zig-zag chains in between the planes of oxygen ions [8]. Thus Al in phase pure boehmite and α-$Al_2O_3$ possesses octahedral coordination while the Al in γ-, δ-, θ-$Al_2O_3$ are in both octahedral and tetrahedral coordination with an increased tetragonal distorted structure; that is in a quasioctahedral coordinated state.

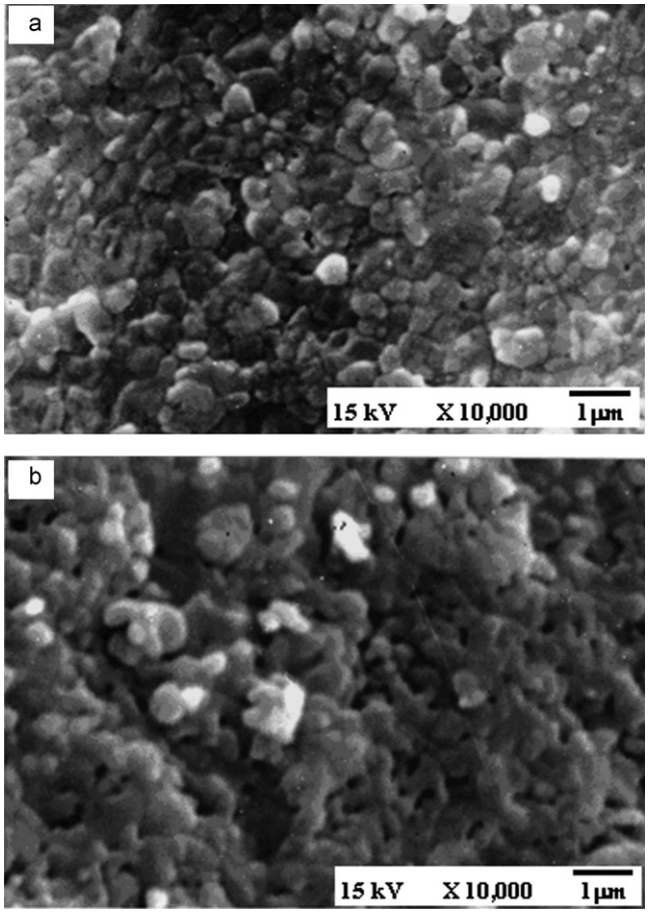


Fig. 8. SEM photographs of sintered alumina at 1500 °C, derived from boehmite precalcined at (a) 400 °C and (b) 1200 °C.

The difference in microstructural features of sintered alumina at 1500 °C, derived from boehmite precalcined at 400 and 1200 °C is presented in Fig. 8. Micrographs presented in Fig. 8a have sub-micron sized grains with sufficient intergranular pores. The grains appear elongated and have nearly uniform size and shape. On the other hand, the micrograph presented in Fig. 8b indicates larger grain size (∼1 μm) with hexagonal to rounded shape. There are also occasional intragranular pores. The increase in density in $P_{1200}$ sintered at 1500 °C is evident from the micrographs.

## 4. Conclusion

As demonstrated, the densification of calcined boehmite gel is very much dependent on the calcination temperature of the sample. The densification is seen to depend on the phases and specific surface area of the precursor and is presumably controlled by cation diffusion. On sintering to 1500 °C, there is a marked improvement in density from 88.2% to 93.1% as the calcination temperature is increased from 400 to 600 °C. The γ-

$Al_2O_3$ present in samples calcined at 600 °C having quasioctahedral coordination and contains cations with high mobility and active sites which improve the densification significantly. In general, the density of sintered product improved on increase in calcination temperature. A maximum of 97.6% of the theoretical density was achieved for boehmite calcined at 1200 °C where octahedral coordination exists when sintered at 1500 °C.

## Acknowledgements

One of the authors Padmaja P. Nampi acknowledges the Council of Scientific and Industrial Research for a Research Fellowship. The technical assistance from P. Krishna Pillai and P. Mukundan is also gratefully acknowledged.

## References

[1] C.W. Turner, Sol–gel process—principles and applications, Ceram. Bull. 70 (1991) 1487–1489.
[2] G.L. Messing, M. Kumagai, Low temperature sintering of α alumina seeded boehmite gels, Am. Ceram. Soc. Bull. 73 (1994) 88–91.
[3] B. Kindl, Y. Liu, E. Nyberg, N. Hansen, The control of interface and microstructure of SiC/Al composites by sol–gel techniques, Compos. Sci. Technol. 43 (1992) 85–93.
[4] Z. Zhang, R.W. Hicks, T.R. Pauly, T.J. Pinnavaia, Mesostructured forms of γ-$Al_2O_3$, J. Am. Chem. Soc. 124 (2002) 1592–1593.
[5] M.M. Amini, M. Mirzaee, Effect of solution chemistry on preparation of boehmite by hydrothermal assisted sol–gel processing of aluminum alkoxides, J. Sol–Gel Sci. Technol. 36 (2005) 19–23.
[6] S.C. Shen, W.K. Ng, Q. Chen, X.T. Zeng, R.B.H. Tan, Novel synthesis of lace-like nanoribbons of boehmite and γ-Alumina by dry gel conversion method, Mater. Lett. 61 (2007) 4280–4282.
[7] S. Komarneni, R. Roy, C.A. Fyfe, G.J. Kennedy, H. Strobl, Solid state $^{27}$A1 and $^{29}$Si magic angle spinning NMR of aluminosilicate gels, J. Am. Ceram. Soc. 69 (1986) C-42–C-44.
[8] W.H. Gitzen (Ed.), Alumina as a Ceramic Material, American Ceramic Society, Inc., Columbus, Ohio, 1970.
[9] B.C. Lippens, J.H. de Boer, Study of phase transformations during calcination of aluminum hydroxides by selected area electron diffraction, Acta Crystallogr. 17 (1964) 1312–1321.
[10] X. Krokidis, P. Raybaud, A.E. Gobichon, B. Rebours, P. Euzen, H. Toulhoat, Theoretical study of the dehydration process of boehmite to γ-Alumina, J. Phys. Chem. B 105 (2001) 5121–5130.
[11] L. Pach, R. Roy, S. Komarneni, Nucleation of alpha alumina in boehmite Gel, J. Mater. Res. 5 (1990) 278–285.
[12] G. Paglia, C.E. Buckley, A.L. Rohl, R.D. Hart, K. Winter, A.J. Studer, B.A. Hunter, J.V. Hanna, Boehmite derived γ-alumina system. 1. Structural evolution with temperature, with the identification and structural determination of a new transition phase, γ′-alumina, Chem. Mater. 16 (2004) 220–236.
[13] A. Boumaza, L. Favaro, J. Ledion, G. Sattonnay, J.B. Brubach, P. Berthet, A.M. Huntz, P. Roy, R. Tetot, Transition alumina phases induced by heat treatment of boehmite: an X-ray diffraction and infrared spectroscopy study, J. Solid State Chem. 182 (2009) 1171–1176.
[14] I. Levin, D. Brandon, Crystal structures and transition sequences, J. Am. Ceram. Soc. 81 (2005) 1995–2012.
[15] H.L. Wen, F.S. Yen, Growth characteristics of boehmite-derived ultrafine theta and alpha-alumina particles during phase transformation, J. Cryst. Growth. 208 (2000) 696–708.
[16] R.S. Zhou, R.L. Snyder, Structures and transformation mechanisms of the structures and transformations mechanisms of the η, γ and θ transition aluminas, Acta Crystallogr. B47 (1991) 617–630.
[17] S. Kwon, G.L. Messing, Constrained densification in boehmite–alumina mixtures for the fabrication of porous alumina ceramics, J. Mater. Sci. 33 (1998) 913–921.
[18] C. Mo, Z. Yuan, L. Zhang, C. Xie, Infrared absorption spectra of nano-alumina, Nanostruct. Mater. 2 (1993) 47–54.
[19] G.K. Priya, P. Padmaja, K.G.K. Warrier, A.D. Damodaran, G. Aruldhas, Dehydroxylation and high temperature phase formation in sol–gel boehmite characterised by FTIR spectroscopy, J. Mater. Sci. Lett. 16 (1997) 1584–1586.
[20] M.H.A.R.M. Ahmad, A.A. Mohamed, A. Ibrahim, C.S. Mahmood, E.G.R. Putra, R. Jamro, R. Kasim, M.R.M. Zin, Microstructural studies of nanocrystalline α-alumina powder produced from $Al_{13}$-cluster, J. Phys. Chem. Solids 68 (2007) 2349–2352.
[21] J.A. Wang, X. Bokhimi, A. Morales, O. Novaro, D.F. Mexico, T. López, R. Gómez, Aluminum local environment and defects in the crystalline structure of sol–gel alumina catalyst, J. Phys. Chem. B 103 (1999) 299–303.
[22] L.A. O'Dell, S.L.P. Savin, A.V. Chadwick, M.E. Smith, $^{27}$Al MAS NMR study of a sol–gel produced alumina: identification of the NMR parameters of the θ-$Al_2O_3$ transition alumina phase, Solid State Nucl. Mag. 31 (2007) 169–173.
[23] B. Kindl, D.J. Carlsson, Y. Deslandes, J.M.A. Haddenbagh, Preparation of α-alumina ceramics: the use of boehmite sols as dispersing agents, Ceram. Int. 17 (1991) 347–350.
[24] H. Nagai, Y. Oshima, K. Hirano, A. Kato, Sintering behaviour of aluminium oxides derived from aluminium hydroxides with various morphologies, Br. Ceram. Trans. 92 (1993) 114–119.
[25] M. Kumagai, G.L. Messing, Controlled transformation and sintering of a boehmite sol–gel by α-alumina seeding, J. Am. Ceram. Soc. 68 (1985) 500–505.
[26] N. Bahlawane, T. Watanabe, New sol–gel route for the preparation of pure alpha-alumina at 950 degrees C, J. Am. Ceram. Soc. 83 (2000) 2324–2326.
[27] V. Vendange, Ph. Colomban, F. Larche, Determination of the hydroxyl content in gels and porous "glasses" from alkoxide hydrolysis by combined TGA and BET analysis, J. Porous Mater. 3 (1996) 196–200.
[28] T.V. Mani, P.K. Pillai, A.D. Damodaran, K.G.K. Warrier, Dependence of calcination conditions of boehmite on the alumina particulate characteristics and sinterability, Mater. Lett. 19 (1994) 237–241.
[29] S. Ghosh, D. Divya, K.C. Remani, T.S. Sreeremya, Growth of monodisperse nanocrystals of cerium oxide during synthesis and annealing, J. Nanopart. Res. 12 (2010) 1905–1911.
[30] A. Pierre, C. Matthieu, Structure and thermal behavior of nanocrystalline boehmite, Thermochim. Acta 425 (2005) 75–89.
[31] J.S. Lu, L. Gao, J.K. Guo, Preparation and phase transition of superfine boehmite powders with different crystallinity, J. Mater. Sci. Lett. 20 (2001) 1873–1875.
[32] G. Paglia, C.E. Buckley, T.J. Udovic, A.L. Rohl, F. Jones, C.F. Maitland, J. Connolly, Boehmite-derived γ-alumina system. 2. Consideration of hydrogen and surface effects, Chem. Mater. 16 (2004) 1914–1923.
[33] A.V. Prasadarao, U. Selvaraj, S. Komarneni, A.S. Bhalla, R. Roy, Enhanced densification by seeding of sol–gel derived aluminum titanate, J. Am. Ceram. Soc. 5 (1992) 1529–1533.